Performance of Graphite Foam Evaporator for Use in Thermal Management

Johnathan S. Coursey

Jungho Kim
e-mail: kimjh@eng.umd.edu

Department of Mechanical Engineering,
University of Maryland,
College Park, College Park, MD 20742

Paul J. Boudreaux
e-mail: pjb@lps.umd.edu
Laboratory for Physical Sciences,
College Park, Maryland 20742

This paper presents the results of an investigation of the thermal performance of a graphite foam thermosyphon evaporator and discusses the foam's potential for use in the thermal management of electronics. The graphitized carbon foam used in this study is an open-cell porous material that consists of a network of interconnected graphite ligaments whose thermal conductivities are up to five times higher than copper. While the bulk graphite foam has a thermal conductivity similar to aluminum, it has one-fifth the density, making it an excellent thermal management material. Furthermore, using the graphite foam as the evaporator in a thermosyphon enables the transfer of large amounts of energy with relatively low temperature difference and without the need for external pumping. Performance of the system with FC-72 and FC-87 was examined, and the effects of liquid fill level, condenser temperature, and foam height, width, and density were studied. Performance with FC-72 and FC-87 was found to be similar, while the liquid fill level, condenser temperature, geometry, and density of the graphite foam were found to significantly affect the thermal performance. The boiling was found to be surface tension dominated, and a simple model based on heat transfer from the outer surface is proposed. As much as 149 W *were dissipated from a* 1 cm^2 *heated area.* [DOI: 10.1115/1.1871193]

Introduction

The electronics market is driven by the desire for increased performance and function along with decreased size. Meeting these demands requires constantly increasing power density. While shifting to lower operating voltages and more efficient circuit designs have helped minimize heat loads, greater performance demands will inevitably lead to higher heat fluxes. High performance heat flux removal technology is necessary to dissipate the generated heat load while maintaining lower operating temperatures, which ensure reliability and result in reduced gate delay and higher processor speed. Typically, 85°C is considered the thermal design temperature limit for high performance memory and logic chips, while higher temperature limits may be appropriate for other devices.

One method of managing a large thermal load is with a thermosyphon, a technology that is now seeing greater application in commercial products. A two-phase closed thermosyphon consists of an evaporator, a condenser, and an adiabatic section that allows a working fluid to travel between the two. Vapor generated at the evaporator rises due to buoyancy forces, and then condenses at the top of the chamber at the condenser, releasing its latent heat. Gravity then returns the condensate back to the evaporator, and the process repeats. Heat generated by a microprocessor could be transferred to the evaporator of a thermosyphon that is bonded with a thin thermally conductive interface to the backside of the chip. At the evaporator, heat would vaporize a working fluid such as one of the fluorinerts FC-72 or FC-87, and ultimately, heat would be dissipated at the condenser.

Much research has been conducted on enhanced evaporators for liquid immersion electronics cooling. In particular, many have studied enhanced copper surfaces. Mudawar and Anderson [1,2] examined the pool boiling performance of fluorinerts on enhanced copper studs and microgrooves and achieved heat fluxes of about 105 W/cm^2 with FC-72 at a superheat of 30°C ($T_{wall} \sim 85°C$). In Ramaswamy et al.'s [3,4] studies of pool boiling FC-72 over an enhanced microstructure thermosyphon made from copper, they achieved heat fluxes up to 100 W/cm^2. In another study, Ramaswamy et al. [5] studied microfabricated silicon evaporators and found that heat transfer increased for increased pore size in the range from 90 to 320 μm. However, the effect of pore density (pores per unit area) was much more significant with higher pore density resulting in higher heat transfer. They also found that increasing the height of the evaporator does not proportionally increase heat transfer because boiling at subsurface layers is largely inhibited compared to the boiling that occurs at the surface.

While many researchers have concentrated on thermosyphon evaporators made from traditional materials, some are now putting emphasis on thermally conductive foams made from metal or graphite. While studying pool boiling of FC-72 over aluminum foam heat sinks, Athreya et al. [6] found that pore density and porosity (fraction of open volume) limit the height of the foam that participates in the nucleate boiling process. In Gulliksen et al.'s [7] study of pool boiling of FC-87 with a porous silver membrane, it was observed that increased permeability of the porous media was key to heat transfer coefficient enhancement.

Another material with great promise for use as a thermosyphon evaporator is graphitized carbon foam. The graphite foam used in this study is mesophase-pitch-derived carbon foam developed by Klett et al. [8]. It is an excellent thermal management material due to its low density, high thermal diffusivity, and a coefficient of thermal expansion that is close to that of silicon. Characteristic properties are shown in Table 1. The open-celled structure (Fig. 1) is easily wetted by FC-72 and FC-87, and the graphitized ligaments provide numerous potential nucleation sites. The primary goal of the study presented here was to evaluate thermal performance and to parametrically study operating conditions and foam characteristics.

Experimental Setup

A diagram of the experimental rig used in this study is shown in Fig. 2. An acrylic chamber was formed by attaching two ring shaped flanges to the cylindrical wall using epoxy. The top and bottom of the chamber were sealed by neoprene o-rings, which were pressed between the polycarbonate lids and the acrylic

Contributed by the Electronic and Photonic Packaging Division for publication in the JOURNAL OF ELECTRONIC PACKAGING. Manuscript received November 13, 2003; revision received June 1, 2004. Review conducted by: K. Kishimoto.

Table 1 PocoFoam™ properties (see Ref. [13])

Property	Value
Pore diameter (average)	350 μm
Specific area	> 4 m^2/g
Open porosity	> 96%
Total porosity	73 – 82%
Density	0.2 – 0.6 g/cm^3
Thermal conductivity	100 – 150 W/(m·K)
Specific heat	0.70 J/(g·K)
Thermal diffusivity	3.71 cm^2/s
Coefficient of thermal expansion	2 – 3 μm/(m·K)
Compressive strength (when density = 0.5 g/cm^3)	2.07 MPa

flanges. Additionally, the center of the chamber base featured another opening, which allowed different samples, surrounded by ceramic insulation (Cotronics™ 914 machinable glass ceramic), to be placed in the chamber. This was then sealed with silicone RTV.

The graphite foam samples were heated by a 1 cm^2 circular heating surface. Heat was provided by a 500 W cartridge heater embedded within an oxygen free high conductivity (OFHC) copper heating block that was insulated with polyurethane foam (not shown in Fig. 2). The neck of the heating block was insulated to create a one-dimensional heat flux. This heat flux and the wall

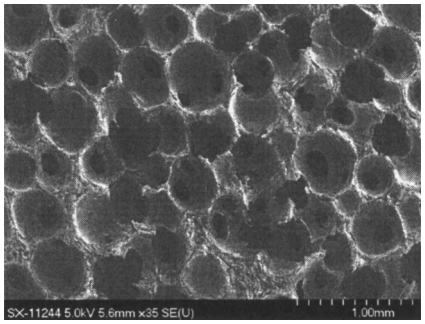

Fig. 1 Scanning electron micrograph of graphite foam [courtesy of James Klett, Oak Ridge National Laboratory]

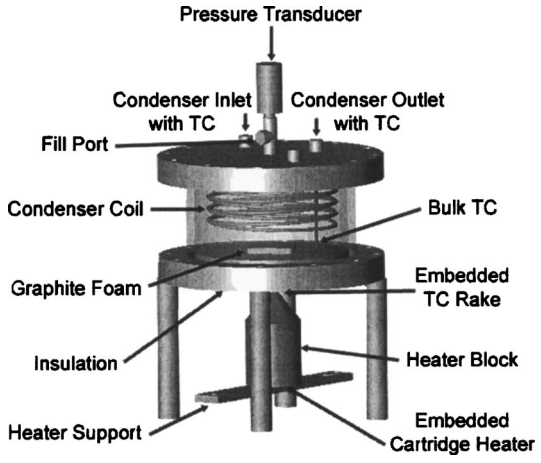

Fig. 2 Experimental setup (TC: thermocouple)

Table 2 Geometry and density of samples studied

Sample Code	Height [cm]	Width [cm]	Width [cm]	Density [g/cm^3]
H-W-D0	0.7	1.25	1.25	0.46
H+W-D0	1.7	1.25	1.25	0.46
H-W+D0	0.7	3.75	3.75	0.46
H0W0D0	1.2	2.50	2.50	0.46
H+W+D0	1.7	3.75	3.75	0.46
H+W+D-	1.7	3.75	3.75	0.33
H+W+D+	1.7	3.75	3.75	0.52
H0W0HTC-	1.2	2.5	2.5	0.68
H0W0HTC+	1.2	2.5	2.5	0.89

temperature were determined from type T thermocouples that were fixed with epoxy into each of three holes (1.3 mm diameter, 6.4 mm separation) located in the neck of the copper column.

The chamber pressure was varied by controlling the temperature of the water inside the copper (alloy C122) condenser coil (0.95 cm outer diameter 0.8 cm inner diameter, 5.5 coils, 195 cm total length). Condensate that formed on the condenser fell back into the pool around the perimeter of chamber keeping subcooled drops far from the graphite foam. A Neslab™ RTE17 constant temperature bath provided a nominally constant condenser temperature, however, the inlet and outlet temperatures of the water in the condenser were continuously measured with type T thermocouples. The chamber pressure was measured by an Omega™ thin-film pressure sensor (PX212-030AV).

Data acquisition and heating control were provided by a VISUAL C++ program through a general programming interface bus on a Pentium III personal computer. An HP6675A direct current power supply provided controllable power, while a Fluke Hydra™ data acquisition unit acquired data from the pressure and temperature channels approximately every 3 s.

Graphite Foam Samples. Large graphite foam blocks from Poco Graphite, Inc.™ were cut and milled into several rectangular samples. The dimensions of the samples are tabulated in Table 2. The sample codes are explained in Table 3. The reasoning behind the choice of these particular samples is given later in the design of experiments discussion.

Bonding Method. In order to effectively use graphite foam as a thermosyphon evaporator, it must be bonded to the heating surface with a low thermal resistivity bond. In this case, the graphite foam had to be bonded to a 1 cm^2 OFHC copper surface. The graphite foam itself is not wetted by conventional solder, but a number of other techniques may be used for bonding.

One method involved electroplating the electrically conductive graphite foam with a thin layer of copper, then bonding that copper surface to the copper heating block with conventional 60/40

Table 3 Explanation of sample codes

Symbol	Explanation
H	Height
W	Width
D	Density
HTC	High Conductivity Foam
-	Low Level
0	Middle Level
+	High Level

Pb/Sn solder. This method was investigated because it relies on readily available materials and can provide a typical solder bondline. However, for the particular processes used, another more conductive bondline was possible.

The method that produced a bond with the least thermal resistance used S-bond Technologies S-bond™ 220. The S-bond™ 220 is a highly conductive fluxless solder that can bond common materials such as copper and aluminum to porous materials such as graphite foam without significant filling of the pores. The bond is made between 250 and 270°C and relies on ultrasonic vibration to break up surface oxides rather than solder flux. To create a stronger and less thermally resistive bond, S-bond™ 220 metallization of graphite in a vacuum furnace was investigated rather than bonding in open air. This work was performed by S-bond Technologies. S-bond™ 220 paste was applied to the bottom surface of the graphite foam, and it was cured at about 850°C in a vacuum furnace. The metallized surface was then soldered to the copper heater block using the same solder but in open air using the low temperature process described earlier. This method was very successful, and it is believed that the thermal resistance of the S-bond™ 220 interface is small. In all cases the thermal resistance of the bondline was considered to be part of the overall thermal resistance of the system being tested.

Working Fluid. Both FC-72 (C_6F_{14}, $T_{sat}=56°C$ at 1 atm) and FC-87 (C_5F_{12}, $T_{sat}=30°C$ at 1 atm) were used in this study. Fluorinerts were investigated because they are thermally and chemically stable dielectric fluids, which are very appropriate for electronics cooling. Furthermore, they are not flammable and are considered nontoxic at temperatures below 200°C. While their very low surface tensions allow them to wet the graphite foam, they unfortunately have low thermal conductivities and latent heats of vaporization. Nevertheless, they are commonly used for thermal management.

System performance was investigated with both fluids, however, the performances were very similar, as will be shown. Given this result and since these fluorinerts are so similar in nature, it was assumed that there is little interaction between the type of fluid (FC-72 or FC-87) and the other parameters of interest. Therefore, only one fluid, FC-87, was used in investigation of the other parameters.

The working fluid was degassed to remove noncondensable gas before each trial by pulling a partial vacuum on the filled chamber. As the fluid boiled due to the low pressure, previously dissolved gas along with some FC vapor was removed by the vacuum pump. This process was repeated until saturated conditions were obtained at room temperature. Under saturated conditions, the chamber pressure is given by the manufacturer's vapor pressure equations, Eqs. (1) and (2) (see Ref. [9]):

$$\log_{10}(P_{v,FC\text{-}72}) = 9.729 - \frac{1562}{T_{\text{bulk}}} \tag{1}$$

$$\log_{10}(P_{v,FC\text{-}87}) = 10.102 - \frac{1548}{T_{\text{bulk}}} \tag{2}$$

where T_{bulk} is in Kelvin and P_v is in Pascal. The bulk temperature near the boiling surface was measured with a "special limits of error," type T, thermocouple probe. This bulk temperature measurement was compared to the saturation temperature calculated by using the measured chamber pressure and Eqs. (1) and (2), and the variation was less than 2°C. In all trials other than the ones designed to test the liquid level effect, the liquid level was 2.0 cm±0.05 cm, as measured from the heated wall.

Design of Experiments. A parametric investigation of performance was performed on the working fluid type, liquid fill level, condenser temperature, and foam density, width, and height. The type of working fluid was investigated with a liquid fill level above the graphite foam sample (2.0 cm) and a condenser at room temperature (25°C). Both the liquid fill level and the temperature of the condenser parameters were varied using only FC-87 as the working fluid since it is believed that these effects would not be dependent on the type of fluorinert used. All three of these operating condition parameters were varied while holding constant the other variables like foam geometry, density, and bonding method. The parametric levels investigated for the operating conditions are shown in Table 4.

Table 4 Range of conditions for operating conditions investigation

Parameter	Level			
Working Fluid	FC-72		FC-87	
Liquid Fill Level [cm]	0.5	1.0	1.5	2.0
Temperature of the Condenser [°C]	20		25	30

The geometry effects, height (along the axis of the copper heater block), and width (perpendicular to the axis of the heater), were studied using a linear with center point experimental design. To study the density effect, the geometry was kept constant at the high levels, while the density was investigated at three levels. These three levels represent samples with midpoints (in terms of height) taken from 1, 2, and 3 cm from the top of the graphite blocks provided by the manufacturer. However, since the density variation of the foam is nonlinear with respect to height, the three levels investigated do not form a linear set of conditions for the parametric investigation of the density factor. The geometry and density parameters were varied while holding constant other variables like operating conditions and bonding method. The levels investigated for geometry and density parameters are shown in Table 5. However, some additional data were obtained for the high thermal conductivity version of the graphite foam (HTC foam) using a different bonding method (copper plating rather than S-bond™). These two HTC samples were taken from the top and bottom of the HTC block provided by the manufacturer. Their results are also presented and support the primary data for the parametric study.

Experimental Procedure. In each trial, the experiment began by supplying the cartridge heater with 20 W of electric power and subsequently monitoring all of the sensors described earlier. Transient data were recorded approximately every 3 s throughout the experiment. When steady-state was reached, 60 s of steady-state data were acquired, yielding approximately 20 data points. The criterion for determination of the steady state was that the time and space averaged temperature in the neck of the heating block as well as the time-averaged readings of all other sensors change by less than 0.1°C [or 690 Pa (0.1 psi) for pressure] over a 60 s period. Transient temperature data for the neck of the heating block confirm that the heat flux was sufficiently steady. After obtaining steady-state data, the power supplied to the cartridge heater was increased by 10 W and the monitoring process continued. Power was incremented and steady-state data taken until the maximum temperature in the neck of the heater block reached 170°C. This temperature limit was required because with the neck of the heater block at 170°C the body of the block is almost 200°C, the hazardous decomposition limit for FC-72 and FC-87.

Table 5 Range of conditions for geometry and density investigation

Parameter	Level		
Foam Height [cm]	0.7	1.2	1.7
Foam Width [cm]	1.25	2.5	3.75
Density [g/cm^3]	0.33	0.46	0.52

In most cases, critical heat flux (CHF) was not reached.

To determine the wall temperature, the temperature gradient in the neck of the heating block was determined by performing a least-squares fit of the temperature measurements from the three thermocouples in the neck and extrapolating to the wall. The heat flux at the wall was determined using Fourier's law with the value for the thermal conductivity of OFHC copper taken from the American Society for Metals' copper handbook [10], which gives a value of 3.91 W/(cm K) at 20°C. The temperature dependence of the thermal conductivity was considered using Hust and Lankford's [11] model with a residual resistivity ratio (RRR) of 42.15. With this RRR (a sample specific property), the Hust and Lankford [11] model yields the same thermal conductivity value as above. An approximate form of the complicated model used is given in Eq. (3):

$$k_{Cu} = 5.6525 \times 10^{-7} T^2 - 8.59 \times 10^{-4} T + 4.113 \qquad (3)$$

The heat flux calculated in this manner was in good agreement with the power input after accounting for small heat losses from the heating block. Assuming a typical natural convection heat transfer coefficient at the bottom surface of the heater and adding the conduction loss through the foam insulation, the heat loss was calculated to be less than about 10% of the power input.

Uncertainty Analysis. All standard deviations given later are stated with 2σ confidence. The standard deviations in the heat flux results were calculated using the sum of squares method. The thermocouples used to measure the heat flux, wall temperature, and condenser temperature were calibrated over the range of 0–100°C in a water bath and were subsequently calibrated from 100 to 170°C in an oven. The resulting standard deviation for these temperature measurements is ±0.2°C for $T \leqslant 100$°C and less than ±0.7°C for $T > 100$°C. The standard deviation of the thermal conductivity of copper is estimated to be 10%. Since the standard deviations of the temperature measurements and the thermal conductivity vary based on the temperature, the standard deviation of the heat flux was calculated for each steady-state point. The maximum standard deviation of the steady-state heat flux was found to be 12.2%, and over all trials, the average standard deviation was found to be 10.4%.

Other uncertainties include the conditions tested and experimental precision. The increasing heat flux and bulk temperature caused the pressure to rise slightly during the experiments, and the small amount of dissolved gas varied between trials. Overall, the pressure for the FC-87 trials was 106.2 kPa±7.6 kPa (15.4 psi±1.1 psi). The deviation of the foam geometry and density from the nominal values also contributed to the precision error. These deviations averaged 2%. Also, any differences in the surface of foam samples would contribute to a precision error due to its effect on bonding and surface boiling. This effect could not be accurately quantified, but may be inferred from the repeated trials.

Results

Working Fluid Effect. The data obtained for the evaporator's boiling performance with FC-72 and FC-87 are shown in Fig. 3. These data, as well as other observations, indicated nominal improvement with the use of FC-87. The similar performance under saturated conditions is due to the similarity of the thermophysical properties (surface tension, latent heat of vaporization, etc.) of the two fluids. The minor performance deviation is not considered significant.

Condenser Temperature Effect. The data which illustrate the condenser temperature effect are shown in Fig. 4. Performance is shown as a function of wall temperature rather than wall superheat because the changing the condenser temperature merely change the saturation temperature, and all trials result in the same boiling curve when plotted as a function of wall superheat. The effect of increasing the condenser temperature is to linearly decrease the heat flux for a given wall temperature as shown in Fig. 5, which shows performance as a function of condenser temperature for various wall temperatures. Any thermosyphon system employed

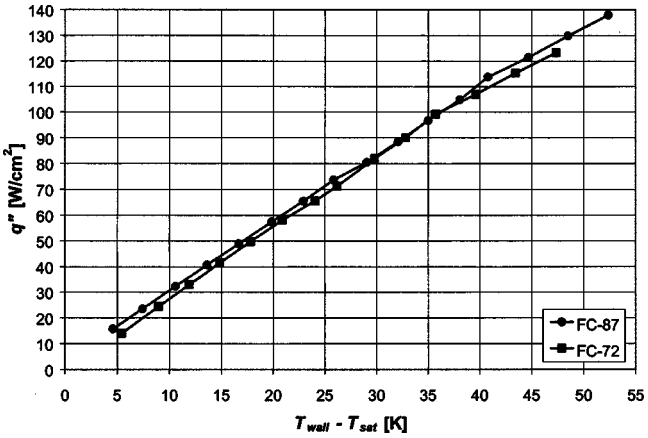

Fig. 3 Boiling curves illustrating the working fluid effect for H=1.2 cm, W=2.5×2.5 cm, ρ=0.89 g/cm³, liquid level=2 cm, T_{cond}=25°C, and copper plate plus Pb/Sn solder

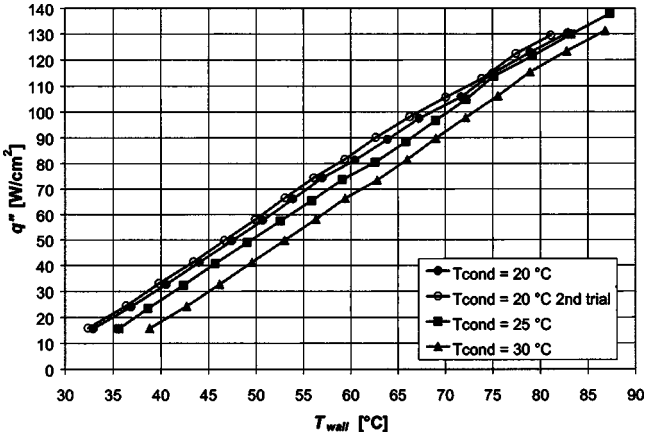

Fig. 4 Boiling curves illustrating the condenser temperature effect for H=1.2 cm, W=2.5×2.5 cm, ρ=0.89 g/cm³, FC-87, liquid level=2 cm, and copper plate plus Pb/Sn solder

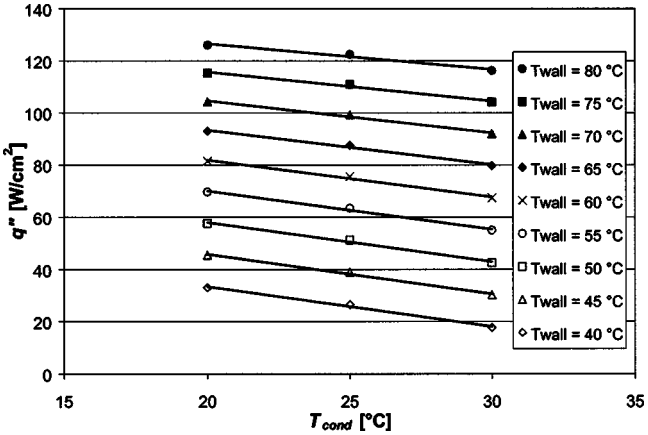

Fig. 5 Condenser temperature effect for H=1.2 cm, W=2.5×2.5 cm, ρ=0.89 g/cm³, FC-87, liquid level=2 cm, and copper plate plus Pb/Sn solder

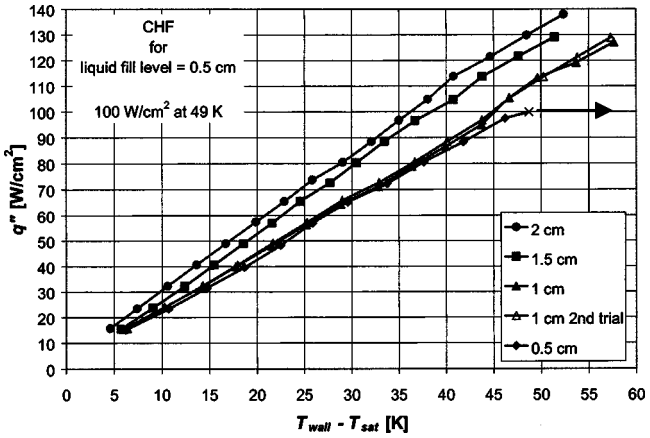

Fig. 6 Boiling curves illustrating the liquid level effect for H =1.2 cm, W=2.5×2.5 cm, ρ=0.89 g/cm^3, FC-87, T_{cond}=25°C, and copper plate plus Pb/Sn solder

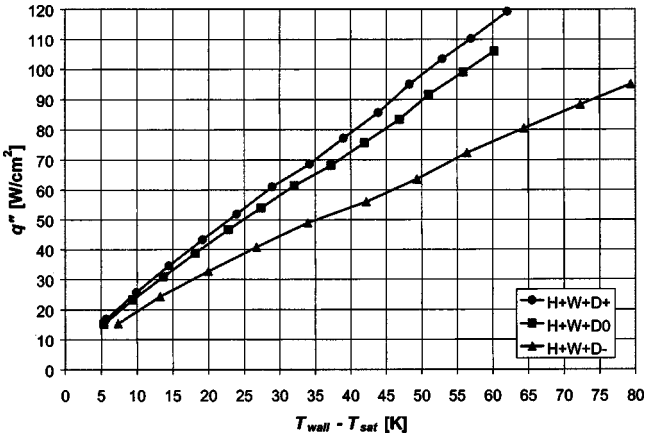

Fig. 8 Boiling curves illustrating the density effect for H =1.7 cm, W=3.75×3.75 cm, FC-87, liquid level=2 cm, T_{cond} =25°C, and S-bond™ 220

to cool electronics should be sized to provide the desired pressure (or T_{sat}) in the system, with lower pressures resulting in higher heat transfer.

Liquid Level Effect. Liquid level can affect the thermal performance of the thermosyphon. Low liquid level can starve the pores of liquid and prevent efficient distribution of liquid within the foam, while an excessively high liquid level can prevent efficient removal of vapor from the surface of the foam. The data obtained for various liquid fill levels are shown in Fig. 6, which shows a significant difference in performance for various liquid fill levels. The lowest liquid fill level of 0.5 cm resulted in premature CHF, while CHF was not observed for the other levels. Though the liquid is wicked into the entire foam due to capillary forces, at lower liquid fill levels only the lower layers of the foam are able to be effectively cooled because cool liquid cannot reach the upper portions of the foam without first going through the hotter lower layers. The result is a decrease in performance due to a decrease in liquid fill level. This effect can be seen clearly in Fig. 7, showing heat transfer as a function of liquid fill level for various wall superheats. Heat transfer is reduced by 27% at a superheat of 10 K and 22% at a superheat of 45 K as the liquid level is decreased from 2 to 0.5 cm. One possible reason that the liquid fill level is less significant at higher superheats is that higher superheats produce more vapor, which entrains liquid and distributes it to the upper regions of the foam.

Density Effect. The data obtained for various graphite foam densities are shown in Fig. 8, which show a significant performance increase for denser foams. This effect can be seen clearly in Fig. 9, which shows heat transfer as a function of foam density for various wall superheats. Figure 9 clearly indicates that the density effect is linear and positive. This effect can be explained by considering the thermal conductivity of the foam, which increases with foam density in a near linear fashion. The higher thermal conductivity of the denser foam allows heat to spread out over a larger area. Spreading the heat farther from the wall results in an increased local superheat and number of active nucleation sites. In this case, increasing the density from 0.33 to 0.52 g/cm^3 resulted in a 52% increase in heat transfer for a superheat of 60 K. Additional data which support these findings and illustrate the density effect for the HTC foam are shown in Fig. 10. Again, increasing density served to spread the heat farther from the wall which increases the local wall superheat. The near linear performance enhancement can be seen clearly in Fig. 11, which shows performance as a function of density for various wall superheats.

Geometry Effects. The data obtained for various graphite foam geometries are shown in Fig. 12. Overall, the best performance was observed for the geometry midpoint, which seems to be a balance between a number of competing mechanisms which are discussed later. The performance of the geometry midpoint indicates a nonlinear effect, and only the two narrow samples reached

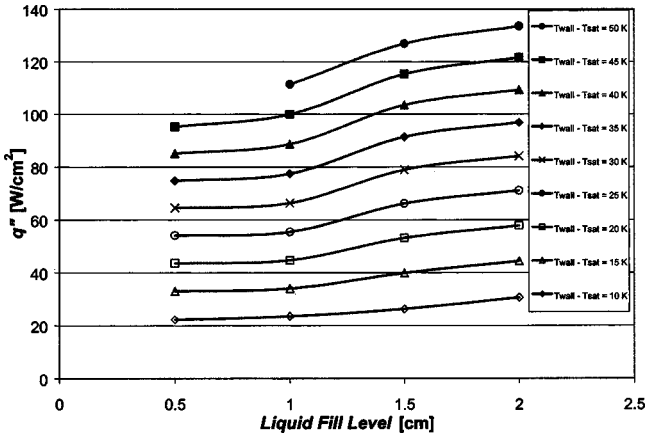

Fig. 7 Liquid fill level effect for H=1.2 cm, W=2.5×2.5 cm, ρ =0.89 g/cm^3, FC-87, T_{cond}=25°C, and copper plate plus Pb/Sn solder

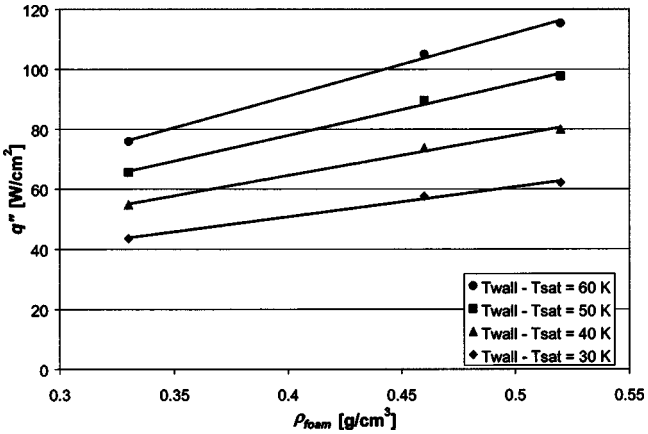

Fig. 9 Density effect for H=1.7 cm, W=3.75×3.75 cm, FC-87, liquid level=2 cm, T_{cond}=25°C, and S-bond™ 220

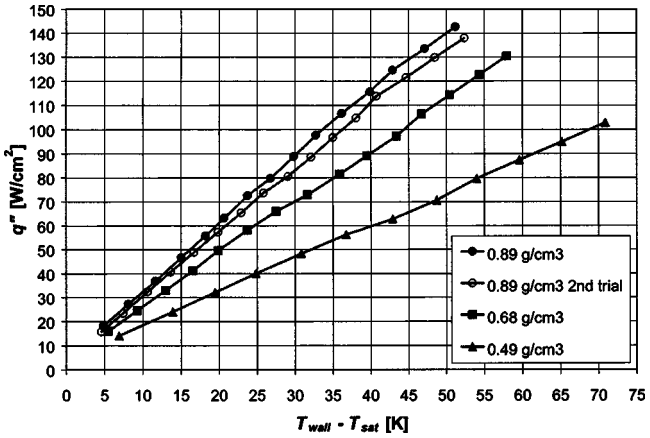

Fig. 10 Boiling curves illustrating the density effect for H =1.2 cm, W=2.5×2.5 cm, FC-87, liquid level=2 cm, T_{cond} =25°C, and copper plate plus Pb/Sn solder

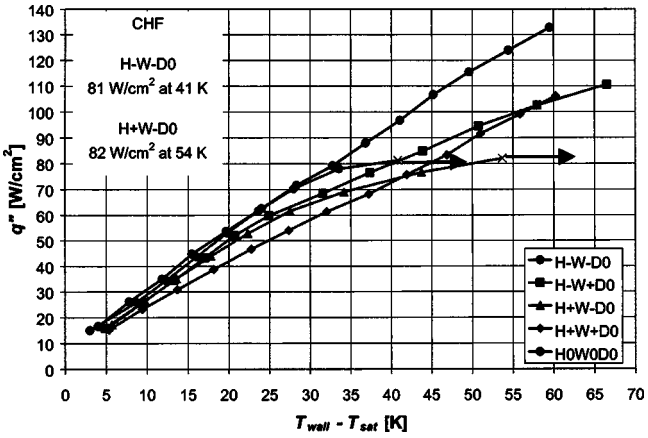

Fig. 12 Boiling curves illustrating the size effects for ρ =0.46 g/cm^3, FC-87, liquid level=2 cm, T_{cond}=25°C, and S-bond™ 220

CHF during the experiments.

The data indicate that wider samples may result in poorer performance at low superheats, but they have higher CHF values. While the boiling area is significantly increased for wider samples, much of this area is too far from the wall to be significant (i.e., there is a fin effect as noted by Ramaswamy et al. [5]).

Mechanisms similar to those governing the width effect also govern the height effect. It was observed that increasing the height beyond a certain value tended to result in lower heat fluxes. Again, the boiling area is increased, providing more potential nucleation sites, but the performance decreases because of another mechanism. This decrease in performance for taller samples may be the result of moving the top surface of the foam farther from the heated wall.

Discussion

There are many factors which determine how the boiling process proceeds inside a conductive foam, but unfortunately, there is no way to actually look inside and observe the process without significantly affecting the process itself. In an attempt to better understand this dynamic heat transfer process, this section presents two analyses on the nature of boiling inside graphite foam. Two of the primary factors controlling the boiling process are the impedance to fluid flow caused by the torturousity of bubbles moving through the connected pores and the temperature distribution throughout the foam. The former factor is analyzed in terms of a dimensionless analysis of the relevant forces, while the latter is analyzed in terms of a fin effect.

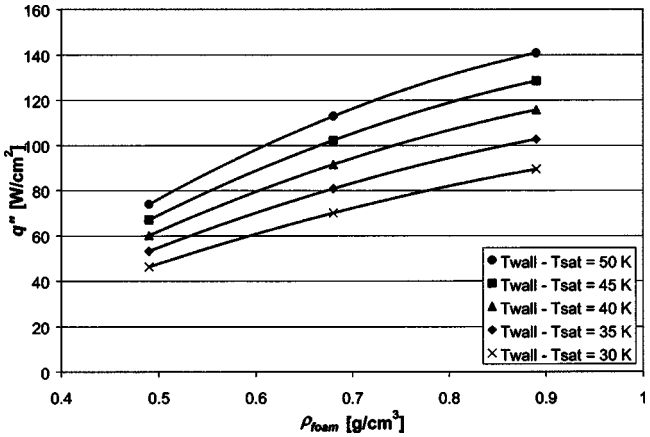

Fig. 11 Density effect for H=1.2 cm, W=2.5×2.5 cm, FC-87, liquid level=2 cm, T_{cond}=25°C, and copper plate plus Pb/Sn solder

Nondimensional Analysis. The bond, capillary, and Grashof nondimensional numbers are useful in providing insight into the balance of forces governing the boiling process [see Eqs. (4)–(6)]:

$$\mathrm{Ca} = \frac{\mathrm{We}}{\mathrm{Re}} = \frac{\mu u}{\sigma} \tag{4}$$

$$\mathrm{Bo} = \frac{g(\rho_l - \rho_v)d_{\mathrm{pore}}^2}{\sigma} \tag{5}$$

$$\mathrm{Gr} = \frac{g\beta(T_{\mathrm{wall}} - T_{\mathrm{sat}})d_{\mathrm{pore}}^3}{\nu^2} \tag{6}$$

Of these, only the bond number can be directly computed from the thermophysical properties. Both the capillary and Grashof numbers rely on the velocity and superheat, respectively. In order to calculate these nondimensional numbers and use them to understand the boiling phenomena, the liquid velocity was calculated for a known wall superheat and heat flux (experimental data).

Data from boiling FC-87 and a high thermal conductivity foam are used in the following calculations. The associated boiling curve is given in Fig. 10. The mass flux can be estimated by assuming all of the heat transferred by the foam is a result of latent heat transfer

$$q = \dot{m}h_{fg} \tag{7}$$

The vapor efflux velocity can be determined using

$$u_{v,l} = \frac{q}{\rho_{v,l}A_c h_{fg}} \tag{8}$$

For a heat dissipation of 142.6 W, wall temperature of 84.6°C, saturation temperature of 33.4°C, and cross-sectional area of 2.5×2.5 cm, the vapor and liquid velocities were calculated to be 20 and 0.1 cm/s, respectively.

Using this liquid velocity and wall superheat, all three nondimensional numbers can be calculated. The bond number, the ratio of buoyancy forces to surface tension forces, was calculated to be 0.22. The capillary number, the ratio of viscous forces to surface tension forces, was calculated to be 6.6×10^{-5}. Finally, the Grashof number, the ratio of buoyancy forces to viscous forces, was calculated to be 443. These dimensionless numbers make it clear that the viscosity of the liquid is of little importance when compared to the buoyancy or surface tension. Furthermore, the low bond number indicates that bubbles would have to overcome

a large surface tension force before departure. This leads to the conclusion that heat transfer is reduced due to a high surface tension force which reduces bubble departure frequency. The notion of a reduction in performance due to high surface tension forces is supported by the literature (e.g., Gulliksen et al. [7]), which indicates that small pores and low permeability reduce heat transfer.

The Fin Effect. Typically, heat transfer coefficients for boiling heat transfer are greater than 2500 $W/(m^2\,K)$. However, even though the graphite foam dissipates a large heat load (>100 W from a 1 cm^2 heating area), the surface area of the foam is enormous (>4 m^2/g). Given this surface area, it appears that the heat transfer from the foam is rather poor, which is typical in systems dominated by surface tension effects. This poor thermal performance can be illuminated by considering the general expression for local convection heat transfer shown in Eq. (9):

$$q''_x = h_x(T_x - T_f) \tag{9}$$

Regardless of the heat transfer coefficient, the local convection heat transfer inside the foam is significantly affected by the temperature difference. Wong and Dybbs [12] found that local thermal equilibrium may exist in liquid saturated porous media. With no significant temperature difference between the solid and fluid phases, there can be no significant convection heat transfer in the foam's interior. The only possible mode of heat transfer from the interior would be latent heat transfer, which occurs at a constant temperature. However, to be significant, latent heat transfer requires a high mass flux. In the case of this pool boiling graphite foam, the dominance of surface tension forces as outlined before ensures a low mass flow rate to and from the foam's interior.

Given no significant convection or latent heat transfer from the interior, a highly simplified but fairly accurate model of thermal performance can be developed by considering the graphite foam as a solid block with the thermal conductivity given by the manufacturer (i.e., a fin subjected to boiling on the surface). In this manner, the data presented in Fig. 10 were used to determine an average local heat transfer coefficient for the graphite foam's outer surface. The temperature drop at the bondline and the solder's affect on thermal conductivity were neglected, and the average heat transfer coefficient on the surface was calculated to range from 2000 to 3000 $W/(m^2\,K)$, depending on superheat. Including the thermal resistance of the bondline would increase the accuracy of the model and result in a slightly higher heat transfer coefficient. This relatively poor boiling heat transfer coefficient is typical for a surface tension dominated system, which supports the validity of the simplified model. This model suggests that even higher heat transfer can be obtained by increasing the surface area of the foam exposed to liquid so boiling occurs over even larger areas. This model also explains why CHF was not observed for most of the samples tested, since the heat flux from the foam's outer surface is low and therefore still within the linear region of the nucleate boiling regime. Tests with enhanced surfaces are currently underway.

Conclusions

The use of graphite foam as the evaporator in a thermosyphon for the cooling of electronics shows significant promise. Evaporator performance with both FC-72 and FC-87 were quite similar. Increasing the liquid fill level was found to increase performance by up to about 25% depending on superheat due to an increase in the wetted area. Increasing condenser temperature decreased performance on a wall temperature basis but had no effect on a wall superheat scale. The geometry of the foam was found to significantly affect heat transfer in a nonlinear manner by changing the boiling area and the distance of this boiling area from the heated wall. Increasing the density of the foam was found to linearly affect heat transfer by changing the superheat at the foam's outer surface through an increased solid thermal conductivity. Nondimensional analysis showed that viscous forces are negligible and that the surface tension force is much greater than the buoyancy force. This indicates that heat transfer may be reduced due to the small size of the graphite pores. The boiling process was modeled by considering the foam as an extended solid surface with all significant heat transfer occurring at the outer surface. In this manner, the average heat transfer coefficient for boiling FC-87 from a graphite foam surface was found to range from 2000 to 3000 $W/(m^2\,K)$ depending on surface superheat. Heat loads as high as 149 W were dissipated from a 1 cm^2 heated area for 52°C wall superheat.

Acknowledgment

The authors would like to thank Bohumil Horácek and Christopher Henry for their valuable suggestions throughout the project. This project was supported by the Laboratory for Physical Sciences under Grant No. MDA90499C2618. The graphite foam samples were provided by Poco Graphite, Inc.™

Nomenclature

A = Area [m^2]
β = Thermal expansion coefficient [K^{-1}]
d = Diameter [m]
g = Acceleration due to gravity [m/s^2]
h = Heat transfer coefficient [$W/(cm^2\,K)$], latent heat [J/kg]
k = Thermal conductivity [$W/(cm\,K)$]
$\dot{m}$ = Mass flow rate [kg/s]
μ = Dynamic viscosity [kg/(m s)]
υ = Kinematic viscosity [m^2/s]
P = Pressure [Pa]
q = Heat [W]
q'' = Heat flux [W/cm^2]
Re = Reynolds number
ρ = Density [kg/m^3, unless otherwise noted as g/cm^3]
σ = Surface tension [N/m]
T = Temperature [K, unless noted as °C]
u = Velocity [m/s]
We = Weber number

Subscripts

bulk = bulk fluid
c = cross-sectional
cond = condenser
f = fluid
fg = liquid/vapor transition
l = liquid
pore = foam pore
sat = saturation
υ = vapor
x = local

References

[1] Anderson, T. M., and Mudawar, I., 1989, "Microelectronic Cooling by Enhanced Pool Boiling of a Dielectric Fluorocarbon Liquid," ASME J. Heat Transfer, **111**, pp. 752–759.
[2] Mudawar, I., and Anderson, T. M., 1993, "Optimization of Enhanced Surfaces for High Flux Chip Cooling by Pool Boiling," J. Electron. Packag. **115**, pp. 89–100.
[3] Ramaswamy, C., Joshi, Y., Nakayama, W., and Johnson, W. B., 1999, "Thermal Performance of a Compact Two-Phase Thermosyphon: Response to Evaporator Confinement and Transient Loads," J. Enhanced Heat Transfer, **6**, pp. 279–288.
[4] Ramaswamy, C., Joshi, Y., Nakayama, W., and Johnson, W. B., 2000, "Combined Effects of Sub-Cooling and Operating Pressure on the Performance of a Two-Chamber Thermosyphon," IEEE Trans. Compon., Packag. Technol., **23**(1), pp. 61–69.
[5] Ramaswamy, C., Joshi, Y., Nakayama, W., and Johnson, W. B., 2003, "Effects of Varying Geometrical Parameters on Boiling from Microfabricated Enhanced

Structures," ASME J. Heat Transfer, **125**, pp. 103–109.
[6] Athreya, B. P., Mahajan, R. L., and Sett, S., 2002, "Pool Boiling of FC-72 Over Metal Foams: Effect of Foam Orientation and Geometry," Proc. of 8th AIAA/ASME Join Thermophysics and Heat Transfer Conference, Jun 24–26, St. Louis, MO, pp. AIAA 2002–3214.
[7] Gulliksen, M., Haugerud, H., and Kristiansen, H., 1999, "Enhanced Boiling Heat Transfer with Porous Silver Coatings for Electronics Cooling," Proc. 5th ASME/JSME Joint Thermal Engineering Conference, Mar. 15–19, San Diego, CA, p. AJTE99-6268.
[8] Klett, J., Hardy, R., Romine, E., Walls, C., and Burchell, T., 2000, "High-Thermal-Conductivity, Mesophase-Pitch-Derived Carbon Foams: Effect of Precursor on Structure and Properties," Carbon, **38**, pp. 953–973.
[9] 3M, 2002, Fluorinert Electronic Liquid FC-72 & FC-87 Product Information.
[10] *ASM Specialty Handbook: Copper and Copper Alloys*, 2001, J. R. Davis, ed., ASM International, Materials Park, OH, p. 453.
[11] Hust, J. G., and Lankford, A. B., 1984, "Thermal Conductivity of Aluminum, Copper, Iron, and Tungsten for Temperatures from 1 K to the Melting Point," NBSIR-84/3007, pp. 1–16.
[12] Wang, K. F. and Dybbs, A., 1976, "An Experimental Study of Thermal Equilibrium in Liquid Saturated Porous Media," Int. J. Heat Mass Transfer, **19**, pp. 234–235.
[13] Poco Graphite Inc., 2000, PocoFoam Product Information.